Light-gated nano-porous polymersomes from stereoisomer-directed self-assemblies

Hui Chen
Beijing University of Chemical Technology and PSL University Paris
Yujiao Fan
PSL University Paris
Xia Yu
Beijing University of Chemical Technology
Vincent Semetey
PSL University Paris
Sylvain Trépout
Institut Curie, Inserm US43 and CNRS UMS2016 https://orcid.org/0000-0002-5822-407X
Min-Hui Li (min-hui.li@chimieparistech.psl.eu)
PSL University Paris https://orcid.org/0000-0001-5367-0348

Article

Keywords: light-gated nano-porous polymersomes, tetraphenylethene, material exchange and transportation, drug carriers, micro/nanoreactors

Posted Date: June 24th, 2020

DOI: https://doi.org/10.21203/rs.3.rs-36308/v1

Abstract

Capsules with holes in the walls exist in natural systems like virus capsids, and in biomimetic systems like immune-stimulating complexes vaccines and liposomes of phospholipids/surfactants mixtures. Structuring pores into stable membrane and controlling their opening are extremely useful for applications that require nano-pores as channels for material exchange and transportation. Polymersomes, which are stable and robust vesicles made of amphiphilic block copolymer, are good candidates for drug carriers or micro/nanoreactors. Engineering structure-inherent and light-gated nano-porous polymersomes is especially appealing, but still unexplored. Here we present these polymersomes made from a polymer including a tetraphenylethene (TPE) in its center. TPE is an emblematic fluorogen with aggregation-induced emission, which possesses two stereoisomers sensitive to photoisomerization. Trans-isomer of the polymer forms classical vesicles, cis-isomer forms cylindrical micelles, while trans/cis mixtures construct perforated vesicles with nano-pores. Under UV light, the classical polymersomes of trans-isomer can be perforated by its cis-counterpart generated from the photoisomerization.

Introduction

Capsules with regularly spaced holes in the walls exist in Nature. For example, many virus capsids have such a structure, where protein units form a rigid frame with holes.[1] In the biomimetic systems like ISCOM (immune-stimulating complexes) vaccines, cage-like structures exhibit also regular holes, but they are formed from small amphiphilic molecules including saponins, phospholipids and cholesterol[2]. Perforated vesicles (also called stomatosomes) made from small amphiphilic molecules were then clearly identified in two-amphiphiles mixtures,[3,4,5,6] such as in cetyltrimethylammonium chloride/egg phosphatidylcholines (C16TAC/EPC) in NaCl aqueous solution. All these two-amphiphiles systems have a common feature: the amphiphile 1 tends to form micelles, whereas the amphiphile 2 favors vesicle formation. The perforated vesicles are evidenced as intermediate structures in the transition from bilayer vesicles to cylindrical micelles with the increase of the ratio of amphiphile 1 over amphiphile 2.[4] Later, supramolecular capsules with nanopores were reported in dumbbell-shaped amphiphiles containing rod-core[7] and in dendritic amphiphiles containing fluorinated-core.[8] In contrast to the multicomponent systems of small amphiphilic molecules, only one amphiphilic dendrimer is necessary to form porous membrane in these systems. The mechanism of their pore formation is more complicated and seems to be closely related to the membrane rigidity.[7,8] It was possible to change the pore size or pore opening/closing in supramolecular capsules by external stimuli like temperature variation.[7] Structuring pores into stable membrane of capsules and controlling their opening are extremely useful for applications that require nano-pores as channels for material exchange and transportation, such as organ-on-chip tissue engineering.[9,10] However, the number of experimental and theoretical researches in perforated vesicles is still limited.

Here we report on the perforated vesicles with nanopores formed from a mixture of stereoisomers of an amphiphilic polymer PEG550-TPE-Chol (M_n = 1510 Da), where the hydrophilic part is poly(ethylene glycol) (PEG550, M_n = 550 Da), and the hydrophobic part is composed of two rigid cores, a tetraphenylethene (TPE) group and a cholesterol (Chol) moiety, and two aliphatic spacers serving as PEG-TPE and TPE-Chol connections (see Fig. 1A and B). From the point of view of materials, capsules with higher molecular weight and rigid cores are more stable and robust than those made from small molecular amphiphiles. The cholesterol moiety is introduced because it is a biocompatible and bio-sourced lipophilic molecule very popular for the core-construction of self-assemblies[11,12]. The role of TPE is three-fold. Firstly, TPE core is a stilbene-type moiety which has structurally distinct and stable *trans* and *cis* stereoisomers (Fig. 1A).[13,14] Thanks to the shape difference between the *trans* and *cis* isomers, their packing parameter is different and stereoisomer-directed self-assembly has been realized: normal vesicles for *trans*-PEG550-TPE-Chol (Fig. 1C), cylindrical micelles for *cis*-PEG550-TPE-Chol (Fig. 1D), and perforated vesicles for *trans/cis* mixture (Fig. 1B). Secondly, the stilbene-type TPE can undergo *trans-cis* photo-activated isomerization under UV illumination.[15] This photo-isomerization (Fig. 2) can make the self-assembly photo-responsive. Under UV illumination of high intensity (15 mW/cm^2), both normal vesicles and cylindrical micelles tend to transform into porous vesicles (Fig. 5), and the design of smart nanostructures is possible. Finally, TPE is a typical aggregation-induced emission (AIE) fluorophore and highly emissive in aggregate states.[16,17] The self-assembled nanomaterials containing TPE exhibit tuneable brightness, high sensitivity and photostability.[18-20] All PEG550-TPE-Chol self-assemblies in this work are highly fluorescent under normal intensity of UV for observation and imaging (typically < 0.5 mW/cm^2). Therefore, the porous polymersomes reported here can provide a deeper insight in this intriguing perforated membrane structure. They may have interesting potential applications as nanoreactors with selective permeability or membranes of separation with selective transport, *etc*. The AIE fluorescence polymersomes and cylindrical polymer micelles may also be advantageous fluorescent systems for application such as bio-imaging and *in vivo* study of drug bio-distribution.

This paper is organized as follows. The synthesis of PEG550-TPE-Chol (without separation of *trans*- and *cis*-isomers during the synthesis), *trans*-PEG550-TPE-Chol and *cis*-PEG550-TPE-Chol will first be described, followed by their characterization including the study of AIE fluorescence property and *trans-cis* isomerization. Then the self-assembly behaviors of *trans*-PEG550-TPE-Chol, *cis*-PEG550-TPE-Chol, and mixtures of *trans*- and *cis*- isomers (with *trans/cis* ratio of 60/40) will be discussed in detail. The studied *trans/cis* mixtures include PEG550-TPE-Chol obtained inherently by synthesis without isomers separation (*trans/cis* ratio = 60/40) and the mixture prepared intentionally by mixing *trans* and *cis* isomers with the same ratio. Finally, the AIE fluorescence of these self-assemblies including cylindrical micelles, nano-porous vesicles and smooth vesicles will be characterized and their morphological changes in response to UV irradiation will be discussed.

Results

Synthesis and characterization of PEG550-TPE-Chol and their stereoisomers

The synthesis of amphiphilic molecules PEG550-TPE-Chol was performed through the synthetic route as shown in Supplementary Scheme S1. Initially, Ti-catalyzed McMurry coupling reaction was employed to provide TPE-2OMe *trans/cis* mixture (Fig. S1). Because *trans*- and *cis*- isomers of TPE-2OMe have nearly identical retardation factor (R_f) on thin-layer chromatography (TLC), they cannot be separated easily by column chromatography. If no separation between *trans*- and *cis*-isomers was made during the whole synthetic procedure, the final product PEG550-TPE-Chol contained nearly the equivalent rate of *trans*- and *cis*-isomers (see Fig. S3 for ^{1}H NMR spectrum, calculated ratio *trans*/*cis* = 60/40, calculation detail will be discussed below).

The *trans*- and *cis*-PEG550-TPE-Chol were then prepared with the separated intermediate derivatives *trans*-TPE-2COOMe and *cis*-TPE-2COOMe, respectively (Fig. 2A and Scheme S2), where two big and polar substituents methyl 6-hexanoate replaced the methyl groups in TPE-2OMe. Indeed, the two isomers of TPE-2COOMe showed different R_f, 0.52 and 0.44, respectively, on TLC using petroleum ether and ethyl acetate (10:1 volume ratio) as eluent solvents (Fig. S10). They were successfully separated by careful column chromatography. The single crystal of the pure isomer with R_f = 0.52 was acquired by slow evaporation of solvents. Its crystal structure was characterized by X-rays diffraction (see Fig. S11 and Table S1). The results clearly show that the functionalized phenyl groups are located on the opposite sides of the central double bond. Unambiguously, the isomer collected firstly in column chromatographic experiment with R_f =0.52 corresponded to the *trans*-TPE-2COOMe. The isomer collected later with R_f =0.44 was *cis*-TPE-2COOMe. Both isomers are very stable and can be stored at room temperature. ^{1}H NMR spectra (Fig. 2A) show clearly the difference of chemical shifts between H_a (H_b) for *trans*-isomer and H_a' (H_b') for *cis*-isomer at δ around 6.6 ppm (6.9 ppm). The *trans*- and *cis*-TPE-2COOMe were then used as starting materials to synthesize corresponding amphiphilic stereoisomers, respectively (see SI and Scheme S2), *via* hydrolysis reaction to get *trans* and *cis*-TPE-2COOH followed by a first esterification reaction with cholesterol and a second esterification with methoxy-poly(ethylene glycol) (mPEG550-OH). The structures of all the compounds were confirmed by ^{1}H NMR, ^{13}C NMR and high-resolution mass spectrometry (HRMS) (Fig. S4-S9, Fig. S12). *Trans*- and *cis*- isomers were stable and maintained their geometry along the synthetic process from TPE-2COOMe to PEG550-TPE-Chol (see Fig. S13 and S14). For the final amphiphilic stereoisomer *trans*-PEG550-TPE-Chol, the ^{1}H NMR analysis detected tiny *cis*-signals of Ha' next to the main *trans*-signals of H_a (Fig. S15 and Fig. 2B). Careful peak integration revealed that the *trans*-PEG550-TPE-Chol contained around 5% of *cis* isomer. The same result was also observed for the *cis*-PEG550-TPE-Chol (Fig. S15 and Fig. 2C), which contained about 5% of *trans* isomer. This small imperfection can be explained as follows. In order to obtain enough final compounds of *trans*- and *cis*-PEG550-TPE-Chol, TPE-2COOMe have been synthesized in great quantity. The large-scale separation of *trans*- and *cis*-TPE-2COOMe by manual column chromatography are not perfect because their R_f values are too close (see Fig. S10) and it is difficult to separate them completely. Nevertheless, we will show hereinafter this trace impurity will not influence the self-assembly behaviors of both *trans*- and *cis*- PEG550-TPE-Chol.

The molecular weight of *trans*- and *cis*- PEG550-TPE-Chol were then analyzed by size exclusion chromatography (SEC) (Fig. S16). Their SEC peaks are well separated, and the elution time of *trans*-isomer is longer than that of its *cis* counterpart. This observation is completely coherent with the fact that the shapes of *trans*- and *cis*- PEG550-TPE-Chol are quite different, even though their molecular weight are the same (M_n = 1510 Da). Because of the presence of TPE moieties, both *trans*- and *cis*-PEG550-TPE-Chol exhibit aggregation-induced emission under UV light around 365 nm. As shown in Fig. S17, they are not fluorescent when they are solubilized in solution of acetone, but highly fluorescent in aggregated states formed from acetone/water mixture.

The possibility to activate the isomerization between two stereoisomers by heating and by UV illumination has been checked. Both isomers are rather thermally stable as shown by ^{1}H NMR spectra in Fig. S18 and Fig. S19. Heating their solution in DMSO up to 70℃ cannot induce *trans*-to-*cis* or *cis*-to-*trans* isomerization. When heating at 120℃ for 24h, only 12-14% of isomerization occurs. Under weak UV light (365 nm, < 0.5 mW/cm^2), both isomers in solution are also stable during normal observation time (in the order of minutes), as shown by ^{1}H NMR spectra in Fig. S20. Typically, the UV light (365 nm) for TLC revealing is ≤ 0.5 mW/cm^2, and that in Spectrofluorometer is 0.25 mW/cm^2. After 2 min of illumination by UV light (365 nm, 0.5 mW/cm^2), no photoisomerization can be detected (Fig. S20). In contrast, photo-isomerization of isomers in solution takes place readily under high UV light as shown by ^{1}H NMR spectra in Fig. 2B and 2C. *Trans* and *cis*-PEG550-TPE-Chol exposed to UV light (365 nm, 15 mW.cm^{-2}) for 2 min undergo already 19% and 25% of isomerization, respectively. After 10 min of illumination, both *trans*-to-*cis* and *cis*-to-*trans* isomerization reach a stationary state with *trans/cis* ratio of 60/40. The *trans*-isomer is in a little excess compared to *cis*- one, because the *trans*-PEG550-TPE-Chol is more photo-stable than the *cis* one and the *cis*-isomer has a faster isomerization rate than that of *trans*-isomer. No significant photo-cyclization was observed for both *cis* and *trans*-PEG550-TPE-Chol after 10 min of illumination (nearly no ^{1}H NMR signals at 6.7 -6.8 ppm).[15,21]

Self-Assembly of *trans*- and *cis*-PEG550-TPE-Chol and their mixtures: vesicles, perforated vesicles and cylindrical micelles

Considering the molecular weight (M_n = 1510 Da) of PEG550-TPE-Chol, which is higher than traditional small amphiphilic molecules like lipids EPC or DHPC, we prepared the vesicles using thin-film hydration method at high temperature (T = 65 °C) to accelerate the sample hydration and polymer self-organization. Typically, the chloroform solution of PEG550-TPE-Chol or their stereoisomer (0.5 *wt*%) was uniformly deposited on the surface of a roughened Teflon plate, followed by drying in vacuum to remove all solvent and to get a thin polymer film. Then the thin film sample was hydrated with deionized water at 65 °C for 48 h in a sealed bottle. We have shown in the above section that the stereoisomers are stable at 70°C for at least 30 min of heating. Here a long heating duration (48h) being used, we first checked if there were any *trans-cis* isomerization of amphiphiles during the self-assembling process. For this purpose, the self-assemblies of *trans*- and *cis*-PEG550-TPE-Chol recovered by freeze-drying was dissolved in deuterated DMSO and analyzed by ^{1}H NMR, respectively. As shown in Fig. S21, the *trans/cis* ratios of both *trans*- and

cis-PEG550-TPE-Chol do not show any change and keep being 95/5 and 5/95, respectively, after the self-assembling process, which prove the absence of the isomerization.

The morphologies and sizes of the self-assemblies were characterized by cryo-electron microscopy (cryo-EM) and dynamic light scattering (DLS). PEG550-TPE-Chol (*trans*/*cis* = 60/40) self-assembled into perforated vesicles, while *trans*-PEG550-TPE-Chol self-assembled into normal vesicles and *cis*-PEG550-TPE-Chol into cylindrical micelles (Fig. 1B, C and D, Fig. S22-24). Their statistical sizes distributions by DLS are shown in Fig. S25, which indicate multimodal size distributions, especially for vesicles of *trans*-isomer with sizes from 80 nm to 5 mm. Indeed, different sizes of vesicles were observed as shown in Fig. S23. Because the DLS analysis is based on spherical models and gives hydrodynamic diameters (D_h) of spherical particles, the data for *cis*-PEG550-TPE-Chol do not reflect the real size of long cylindrical micelles. The length of cylindrical micelles reaches several hundreds of nanometers until several micrometers, and some closed loops are also visible (see Fig. S24). Note that the trace amount of *cis*-isomer (5%) in the *trans*-PEG550-TPE-Chol did not influence the formation of vesicles, which represent the absolute majority of the morphologies. Meanwhile, *cis*-PEG550-TPE-Chol formed only cylindrical micelles despite the presence of 5% *trans*-isomer according to the collected cryo-EM images. The membrane thickness of vesicles and the diameter of cylindrical micelles were evaluated from the FWHM (Full Width at Half Maximum) of the electronic density profile perpendicular to the membrane through statistical analysis of about 30 different vesicles in the cryo-EM images. The thickness of vesicle membrane for *trans*-PEG550-TPE-Chol was measured as 7.5 ± 0.5 nm, the diameter of cylindrical micelles for *cis*-PEG550-TPE-Chol as 6.5 ± 0.5 nm and the thickness of the membrane of perforated vesicles for PEG550-TPE-Chol as 7.3 ± 0.5 nm.

When the stereo-structure changes from *trans*- to *cis*-type, the morphological transition of self-assemblies from vesicles to cylindrical micelles should be driven by the minimization of the interfacial energy. Following qualitatively the theory of Israelachvili *et al.*[22,23], the packing parameter $p = v/al$ of *trans*-PEG550-TPE-Chol in aqueous solution should be around 1 for vesicle formation, while the p value of *cis*-PEG550-TPE-Chol should be smaller and approach 1/2 for cylindrical micelle formation (where v is the hydrophobic volume, a the optimal interfacial area, and l the length of the hydrophobic block normal to the interface). Here, the chemical structures are the same for both isomers, so their steric shapes dictate their packing parameter in the self-assemblies. A schematic representation of their self-assembly and packing is given in Fig. 3A and 3B. The plausible molecular models of the hydrophobic part for *trans*- and *cis*-PEG-TPE-Chol in the bilayer membranes and cylindrical micelles are illustrated in Fig. S26, with the lengths of l_{trans} = 4.54 nm and l_{cis} = 4.05 nm. The thickness of vesicle membrane (e = 7.5 nm) is between l_{trans} (4.54 nm) and $2l_{trans}$ (9.08 nm), the diameter of cylindrical micelles (d_c = 6.5 nm) is also between l_{cis} (4.05) and $2l_{cis}$ (8.10 nm). Therefore, both *trans*- and *cis*-PEG-TPE-Chol in the bilayer membrane and in the cylindrical micelles should be packed in the interdigitated way as shown in Fig. 3A and 3B. Cholesterol is a versatile building block which supports the formation of bilayer membranes[24] and fibril structures[25,26] due to its molecular rigidity, self-assembling nature, asymmetric carbons, *etc*. For the

cylindrical micelles formed by *cis*-PEG-TPE-Chol, along the cylindrical axis the cholesterol moieties turn around this axis to form the cylindrical micelles, whose cross-section is round as shown in Fig. S24.

Interestingly the PEG550-TPE-Chol forms perforated membranes and vesicles (see Fig. 1B and Fig. S22), similarly to the mixture of small molecular amphiphiles, *e.g.,* C16TAC and EPC.[3] The novelty here is the PEG550-TPE-Chol is a stereoisomers-mixture synthesized as one compound, simply and inherently without the tedious separation of intermediates *trans*- and *cis*-isomers during the synthetic procedure. Further, we prepared artificially the mixtures of both stereoisomers to get *trans*/*cis* ratio of 60/40, the same as inherently synthesized PEG550-TPE-Chol, and then performed the self-assembling by film hydration in the identical conditions. Fig. 4 shows the representative morphologies of its self-assemblies observed by cryo-EM, which are the same as those obtained with inherently synthesized PEG550-TPE-Chol (Fig. 1B).

The scenario of porous membrane formation can be explained as follows. Micelle-forming *cis*-isomers in a bilayer membrane try to impose a positive curvature on the constituent monolayers (leaflets). The monolayers may remain united to a flat bilayer only up to a critical concentration of the micelle-forming *cis*-isomers. Above this critical point, edges may form, which would contain predominately the micelle-forming *cis*-isomers and assemble into hemicylindrical structures with a negative curvature (the holes). With *trans*/*cis* ratio of 60/40, the hole part and strand part have similar proportion in the mesh-like membrane. Table 1 summarizes the measured values for bilayer membrane thickness (e), cylindrical micelle diameters (d_c), pore diameter (d_h) and the minimal wall thickness (e_w) between two pores (see Fig. 4 for the definition). We found $e_w \geq d_c$, which means the narrowest place of the wall is almost composed of the cross-section of two face-to-face hemicylinders.

Table 1. Size characterization of different morphologies of *trans*-/*cis* isomers and mixtures by cryo-EM

Sample	Membrane thickness e(nm)	Cylindrical micelle diameter d_c (nm)	Pore diameter d_h(nm)	Pore wall thickness e_w(nm)
trans-PEG550-TPE-Chol (*trans*/*cis* = 95/5)	7.5 ± 0.5	-	-	-
Isomers mixture (*trans*/*cis* = 60/40)	7.3 ± 0.5	-	9.0 – 27.0	6.9 – 7.6
cis-PEG550-TPE-Chol (*trans*/*cis* = 5/95)	-	6.5 ± 0.5	-	-

AIE and photo-responsive properties of vesicles, perforated vesicles, and cylindrical micelles

All self-assemblies of both *trans*- and *cis*-PEG550-TPE-Chol, as well as of their mixtures are fluorescent under UV light because of TPE moieties. Once the TPE self-assembled in hydrophobic domain of nanostructures, the physical constraints and space limitations enable to restrict the intramolecular rotation of phenyl groups around the singles bonds in TPE. Under UV illumination, the non-radiation decay of excited TPE is locked and the radiative decay channel turns on, consequently nanostructures

become efficiently emissive. Their UV-visible absorption spectra and fluorescence spectra are shown in Fig. 5. The quantum yields are 0.12 and 0.15 for *trans*- and *cis*-PEG550-TPE-Chol assemblies, respectively.

Since both *trans*- and *cis*- isomers can undergo *trans*-to-*cis* and *cis*-to-*trans* isomerization under UV illumination, we have also studied the morphological transformation of their self-assemblies under UV light of higher intensity. Typically, the aqueous dispersions of self-assemblies of *trans*- and *cis*-PEG550-TPE-Chol were exposed to UV light (365 nm, 15 $mW.cm^{-2}$) for 30 min, respectively. One part of the irradiated sample was investigated by cryo-EM, and the rest was first freeze-dried and then solubilized in $CDCl_3$ for analysis by ^1H NMR. ^1H NMR spectra (Fig. S27) show that after UV illumination, the *trans/cis* ratios in both samples become 60/40, in agreement with the results obtained in solution samples exposed to UV light (Fig. 2B and 2C). It is also notable that photocyclization of TPE moiety begin to occur as a trace of new peak emerged at 6.7 -6.8 ppm for both *cis* and *trans*-PEG550-TPE-Chol after 30 min illumination (Fig. S27). Cryo-EM images of both UV treated samples are shown in Fig. 5C and 5D as well as in Fig. S28 and S29. Vesicles of *trans*-PEG550-TPE-Chol initially with homogeneous and smooth surface were perforated by the *cis*-isomers resulted from the photoisomerization, while cylindrical micelles of *cis*-PEG550-TPE-Chol under UV interweaved to form meshes and perforated membranes because of the appearance of *trans*-isomers. The perforated membranes obtained from cylindrical micelles were less structured (Fig. 5D) than those from smooth vesicles, probably for the kinetic reason, *i.e.,* because of the slow rate of the fusion between separated cylindrical micelles. As expected, perforated vesicles and membranes of PEG550-TPE-Chol did not show significant change upon UV light exposure (see cryo-EM images in Fig. S30), because of simultaneous *trans*-to-*cis* and *cis*-to-*trans* isomerization.

Big morphologies like giant vesicles and large membranes also co-existed with nanostructures in PEG550-TPE-Chol self-assemblies as shown in Fig. 4 (and Fig. S22-23, S28-S30). Cryo-EM allows to detect the nanostructures in detail, but it cannot visualize the giant structures wholly. Therefore, epifluorescence optical microscopy was also used for observation of the giant vesicles formed by PEG550-TPE-Chol (Fig. 6). Under UV light, giant vesicles are cyan fluorescent as shown in Fig. 6. With the increase of UV illumination time, the membrane becomes fluctuating, probably because the hole parts and strand parts interchange continuously resulting from the simultaneous *trans-cis* and *cis-trans* isomerization in PEG550-TPE-Chol. Even with this high intensity UV of 15 mW/cm^2, the fluorescence intensity only decreased, but not quenched, after 2 min of illumination (Fig. 6 and Fig. S31), demonstrating good photostability of AIE polymersomes. Further, the fluorescence will be greatly decreased after 60 min illumination due to the cyclization[21] of the TPE moiety (Fig. S31-32).

Discussion

We have shown stereoisomer-directed self-assemblies: *trans*-PEG550-TPE-Chol formed normal vesicles, *cis*-PEG550-TPE-Chol formed cylindrical micelles, and PEG550-TPE-Chol synthesized without isomers' separation (*trans/cis* = 60/40) formed perforated vesicles and membranes with the pores size of 9 - 27

nm. Similar nano-porous vesicles were also obtained by self-assembling the artificial mixture of *trans*- and *cis*-PEG550-TPE-Chol in the ratio of *trans/cis* = 60/40.

All these self-assemblies exhibited AIE fluorescence under UV illumination of normal intensity for observation and imaging (typically < 0.5 mW/cm^2). With stronger UV intensity (15 mW/cm^2) and longer illumination time (2 – 30 min), photo-responsive features were recorded due to *trans*-to-*cis* and *cis*-to-*trans* photo-isomerization. Smooth vesicles of *trans*-PEG550-TPE-Chol were perforated by the *cis*-isomers stemmed from the photoisomerization, while cylindrical micelles of *cis*-PEG550-TPE-Chol interweaved to form meshes and perforated membranes. Nano-porous vesicles of PEG550-TPE-Chol upon strong UV light exposure did not show significant change in nanoscale, but in micrometer scale membrane fluctuation was observed by epifluorescence microscopy.

The vesicles of *trans*-PEG550-TPE-Chol can be considered as light-gated polymersomes, where pores of 9-27 nm were generated under strong UV illumination (15 mW/cm^2). It can be used to perform traced transportation under weak UV light and controlled release of small molecules (< 30 nm) under stronger UV light. Nano-porous polymersomes and polymer membranes are also promising for applications that require nano-pores as channels for material transportation. We speculate that the nano-porous polymersomes may be used as capsules for the culture of multicellular spheroids which are considered as good *in-vitro* models of micro-tissues like tumors or neurons[10,27]. All nutrients (proteins and oxygen) required for cell division can diffuse freely through the capsule membrane and allow proliferation of the encapsulated cells. Meanwhile, since PEG is by nature cell-repellent, cells form cellular aggregates, *i.e.*, multicellular spheroids. Organ-on-chip tissue engineering may be possible using these nano-porous giant polymersomes.

Declarations

Acknowledges

This work was financially supported by the French National Research Agency (ANR-16-CE29-0028). Yujiao Fan gratefully acknowledges the China Scholarship Council for funding her PhD scholarship. We thank Prof. Ben Zhong Tang from Hong Kong University of Science & Technology for fruitful discussions and Dr. Patrick Keller from Institut Curie for critical reading of the manuscript. The PICT-IBiSA of Institut Curie is acknowledged for providing access to cryo-EM facility in Orsay.

Author Contributions

The manuscript was written through contributions of all authors. H.C. and M.-H.L. designed research; H.C., Y.F., Y.X. and M.-H.L. performed research; H.C. and S.T contributed to the cryo-EM imaging and analyses; Y.F. and V.S. contributed to the observation by fluorescent microscopy. H.C. and M.-H.L. analyzed data and wrote the paper.

Corresponding Author

* Min-Hui LI

Email: min-hui.li@chimieparistech.psl.eu

Competing and financial interests: The authors declare no competing financial interests

References

1 Angelescu, D. G. & Linse, P. Viruses as supramolecular self-assemblies: modelling of capsid formation and genome packaging. *Soft Matter* **4**, 1981-1990 (2008).

2 Myschik, J. *et al.* On the preparation, microscopic investigation and application of ISCOMs. *Micron* **37**, 724-734 (2006).

3 Edwards, K., Gustafsson, J., Almgren, M. & Karlsson, G. Solubilization of lecithin vesicles by a cationic surfactant: intermediate structures in the vesicle-micelle transition observed by cryo-transmission electron microscopy. *J. Colloid Interface Sci.* **161**, 299-309 (1993).

4 Almgren, M. Stomatosomes: perforated bilayer structures. *Soft Matter* **6**, 1383-1390 (2010).

5 Ljusberg-Wahren, H. *et al.* in *The Colloid Science of Lipids* (Springer, 1998).

6 van Dam, L., Karlsson, G. & Edwards, K. Direct observation and characterization of DMPC/DHPC aggregates under conditions relevant for biological solution NMR. *BBA-Biomembranes* **1664**, 241-256 (2004).

7 Kim, J. K., Lee, E., Lim, Y. b. & Lee, M. Supramolecular capsules with gated pores from an amphiphilic rod assembly. *Angew. Chem. Int. Ed.* **47**, 4662-4666 (2008).

8 Berlepsch, H. v. *et al.* Controlled self-assembly of stomatosomes by use of single-component fluorinated dendritic amphiphiles. *Soft matter* **14**, 5256-5269 (2018).

9 Alessandri, K. *et al.* A 3D printed microfluidic device for production of functionalized hydrogel microcapsules for culture and differentiation of human Neuronal Stem Cells (hNSC). *Lab Chip* **16**, 1593-1604 (2016).

10 Alessandri, K. *et al.* Cellular capsules as a tool for multicellular spheroid production and for investigating the mechanics of tumor progression *in vitro*. *PNAS* **110**, 14843-14848 (2013).

11 Piñol, R. *et al.* Self-assembly of PEG-b-liquid crystal polymer: the role of smectic order in the formation of nanofibers. *Macromolecules* **40**, 5625-5627 (2007).

12 Zhou, Y., Briand, V. A., Sharma, N., Ahn, S.-k. & Kasi, R. M. Polymers comprising cholesterol: synthesis, self-assembly, and applications. *Materials* **2**, 636-660 (2009).

13 Xie, Y. & Li, Z. Recent advances in the Z/E isomers of tetraphenylethene derivatives: stereoselective synthesis, AIE mechanism, photophysical properties, and application as chemical probes. *Chem. Asian J.* **14**, 2524-2541 (2019).

14 Peng, H.-Q. *et al.* Dramatic differences in aggregation-induced emission and supramolecular polymerizability of tetraphenylethene-based stereoisomers. *J. Am. Chem. Soc.* **139**, 10150-10156 (2017).

15 Bunker, C. E., Hamilton, N. B. & Sun, Y. P. Quantitative application of principal component analysis and self-modeling spectral resolution to product analysis of tetraphenylethylene photochemical reactions. *Anal. Chem.* **65**, 3460-3465 (1993).

16 Mei, J. *et al.* Aggregation-induced emission: the whole is more brilliant than the parts. *Adv. Mater.* **26**, 5429-5479 (2014).

17 Mei, J., Leung, N. L., Kwok, R. T., Lam, J. W. & Tang, B. Z. Aggregation-induced emission: together we shine, united we soar! *Chem. Rev.* **115**, 11718-11940 (2015).

18 Li, J. *et al.* Supramolecular materials based on AIE luminogens (AIEgens): construction and applications. *Chem. Soc. Rev.* **49**, 1144-1172 (2020).

19 Yan, L., Zhang, Y., Xu, B. & Tian, W. Fluorescent nanoparticles based on AIE fluorogens for bioimaging. *Nanoscale* **8**, 2471-2487 (2016).

20 Feng, G. & Liu, B. Aggregation-induced emission (AIE) dots: Emerging theranostic nanolights. *Acc. Chem. Res.* **51**, 1404-1414, doi:10.1021/acs.accounts.8b00060 (2018).

21 Zhu, L. *et al.* Aggregation-induced emission and aggregation-promoted photo-oxidation in thiophene-substituted tetraphenylethylene derivative. *Chem. Asian J.* **11**, 2932-2937 (2016).

22 Antonietti, M. & Förster, S. Vesicles and liposomes: a self-assembly principle beyond lipids. *Adv. Mater.* **15**, 1323-1333 (2003).

23 Israelachvili, J. N., Mitchell, D. J. & Ninham, B. W. Theory of self-assembly of hydrocarbon amphiphiles into micelles and bilayers. *J. Chem. Soc. Faraday Trans.* **72**, 1525-1568 (1976).

24 Echegoyen, L. E. *et al.* The first evidence for aggregation behavior in a lipophilic [2.2. 2]-cryptand and in 18-membered ring steroidal lariat ethers. *Tetrahedron Lett.* **29**, 4065-4068 (1988).

25 Murata, K. *et al.* Thermal and light control of the sol-gel phase transition in cholesterol-based organic gels. Novel helical aggregation modes as detected by circular dichroism and electron microscopic observation. *J. Am. Chem. Soc.* **116**, 6664-6676 (1994).

26 Jung, J. H., Shinkai, S. & Shimizu, T. Nanometer-level sol− gel transcription of cholesterol assemblies into monodisperse inner helical hollows of the silica. *Chem. Mater.* **15**, 2141-2145 (2003).

27 Simkiss, K. & Wilbur, K. M. *Biomineralization*. (Elsevier, 2012).

Additional Files

Supplementary information. ^{1}H NMR and ^{13}C NMR spectra of all compounds. SEC spectra of the synthesized *trans*- and *cis*- PEG550-TPE-Chol. The crystal data and structure of *trans*-TPE-2COOMe. Supplemental data of photoluminescence spectra. Supplemental data of DLS. Supplemental cryo-EM images of the assemblies.

Supplementary Movie*. Movie of giant polymersomes under continuous UV illumination recorded with epifluorescence optical microscope.

*The movie file is not available in this version of the paper.

Figures

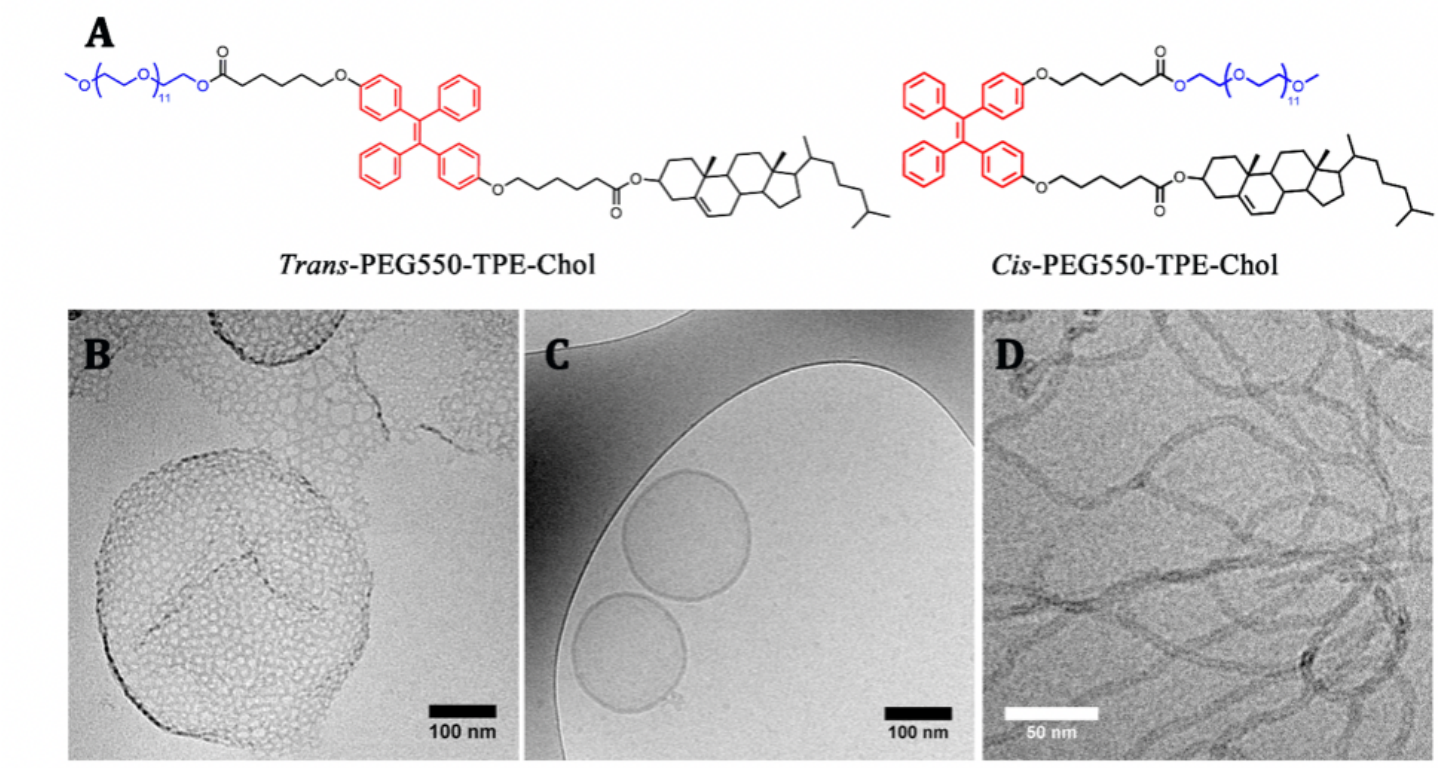

Figure 1

(A) Chemical structures of the two stereoisomers trans-PEG550-TPE-Chol and cis- PEG550-TPE-Chol. (B) Cryo-EM image of porous vesicles formed by PEG550-TPE-Chol synthesized with inherent ratio of

trans/cis = 60/40 without isomers separation (simply noted as PEG550-TPE-Chol in the text). (C) Cryo-EM image of classical vesicles formed by trans-PEG550-TPE-Chol. (D) Cryo-EM image of cylindrical micelles formed by cis-PEG550-TPE-Chol. The method of thin-film hydration was used to perform the self-assembly.

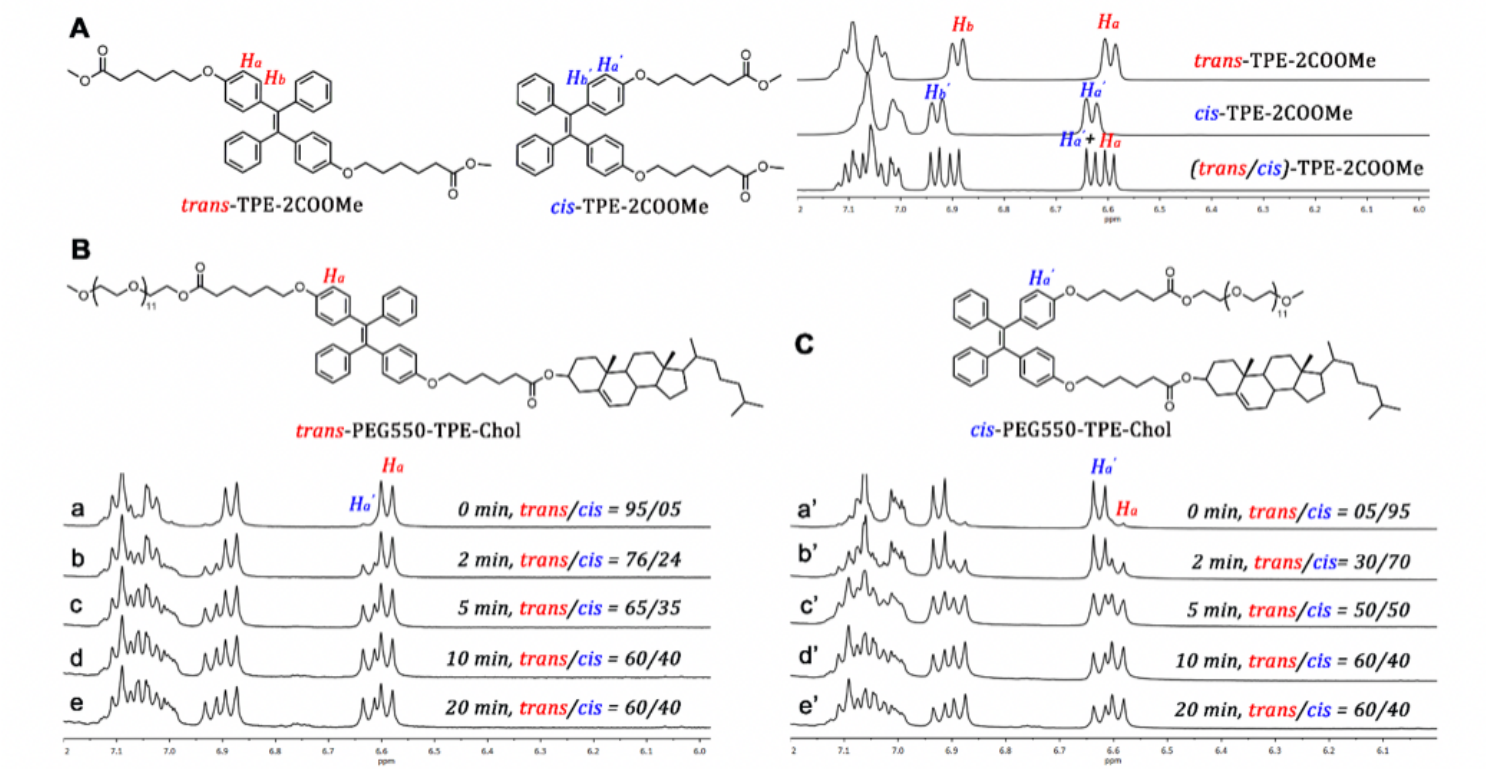

Figure 2

(A) Chemical structure of trans-TPE-2COOMe and cis-TPE-2COOMe and the partial 1H NMR spectra of the trans-TPE-2COOMe, cis-TPE-2COOMe and (trans/cis)-TPE-2COOMe mixture (400 MHz, CDCl3). (B) Chemical structure of trans-PEG550-TPE-Chol, and partial 1H NMR spectra of trans-PEG550-TPE-Chol in CDCl3 after UV irradiation (365 nm, 15 mW/cm2) with different duration: (a) t = 0 min, (b) t = 2 min, (c) t = 5 min, (d) t = 10 min, (e) t = 20 min. (C) Chemical structure of cis-PEG550-TPE-Chol, and partial 1H NMR spectra of cis-PEG550-TPE-Chol in CDCl3 after UV irradiation (365 nm, 15 mW/cm2) with different duration: (a') t = 0 min, (b') t = 2 min, (c') t = 5 min, (d') t = 10 min, (e') t = 20 min. The abscises of all NMR spectra are scaled from 6.0 to 7.2 ppm for clarity.

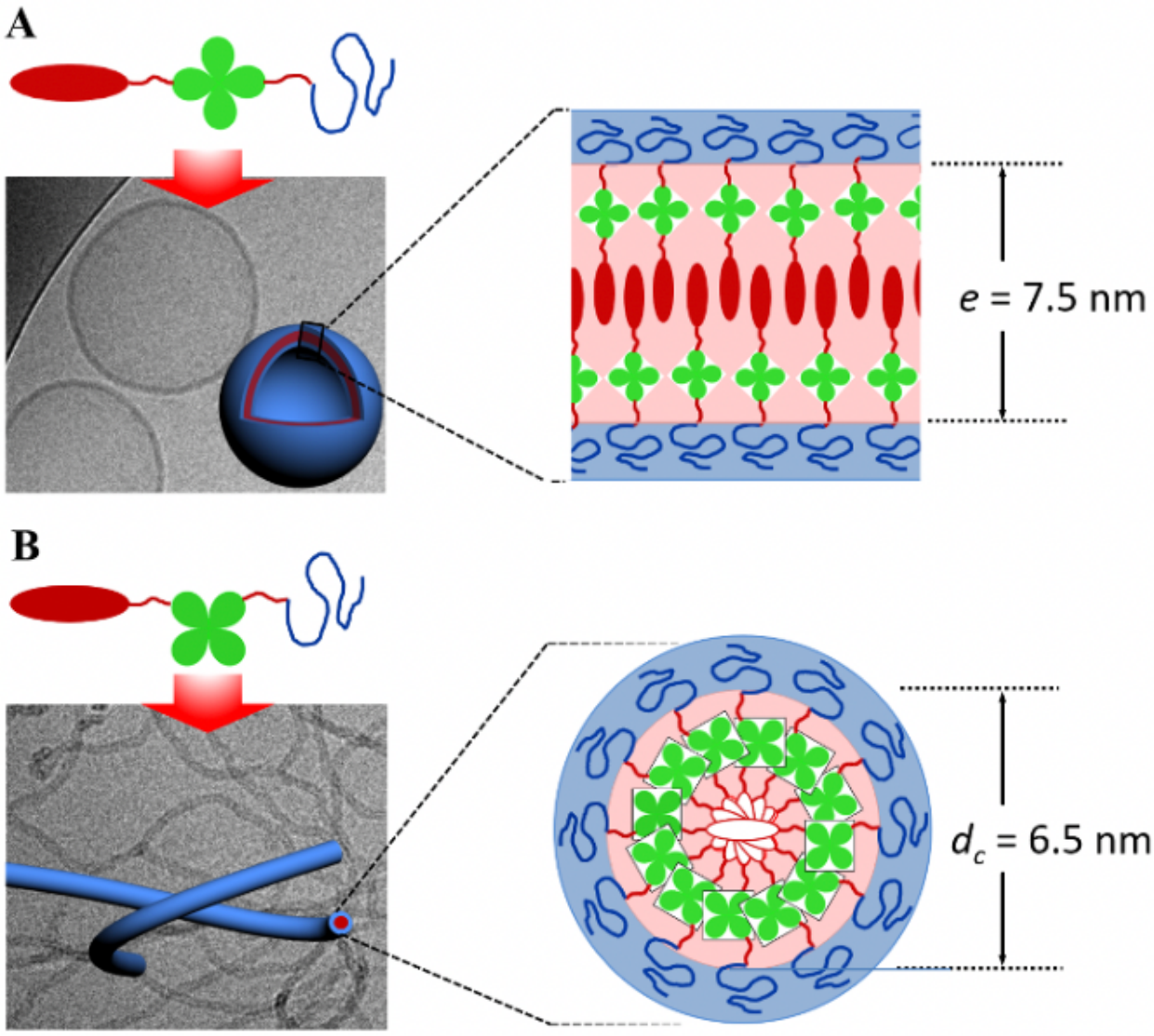

Figure 3

The morphologies models of polymersomes (A) and cylindrical micelles (B) formed by trans-isomer and cis isomer, respectively. The red ellipsoid represents the cholesterol moiety, and the green trefoil the TPE group. The red line represents the aliphatic spacer, and the blue line the PEG550 chain. In the cylindrical micelle model, empty red ellipsoids are used to represent the cholesterol moiety in order to highlight molecular organization along the cylinder long axis.

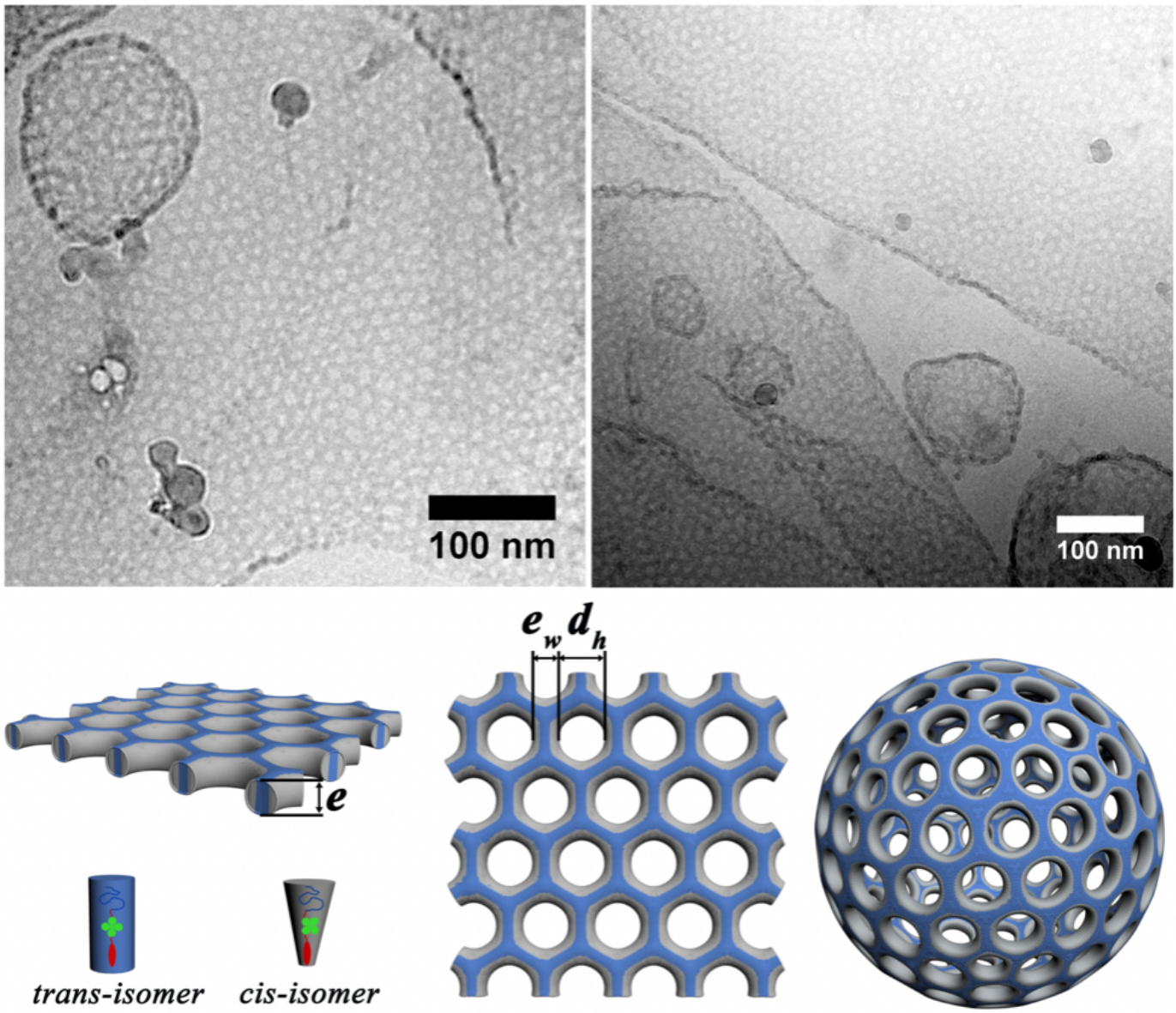

Figure 4

Cryo-EM images of self-assemblies obtained from trans- and cis-PEG550-TPE-Chol mixtures (trans/cis = 60/40), and schematic representation of perforated membrane and nano-porous polymersomes.

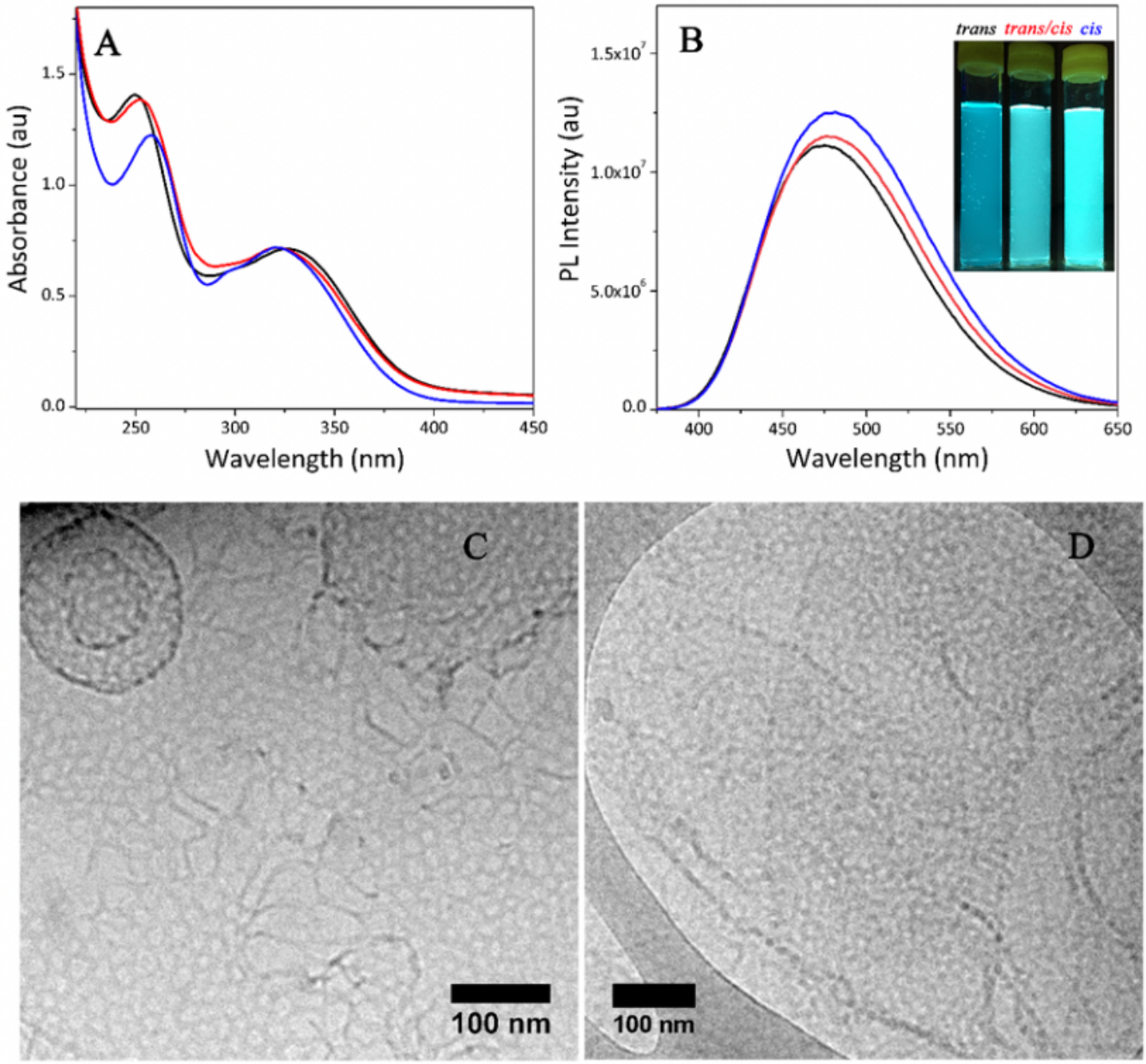

Figure 5

(A) The UV-visible absorption spectra of trans assemblies (black line), cis assemblies (blue line) and the assemblies formed by trans/cis mixtures (trans/cis = 60/40) (red line). (Concertration: 6,7 x10-2 mg/ml). (B) The photoluminescence (PL) spectra of trans assemblies (black line), cis assemblies (blue line) and the assemblies formed by trans/cis mixtures (trans/cis = 60/40) (red line). (concentration: 6.7 × 10−2 mg/ml; excitation wavelength: 352 nm, 0.5 mW/cm2). The inset photos are the dispersions of self-assemblies taken under 365 nm UV light (0.5 mW/cm2). (C) and (D) Cryo-EM images of perforated membranes and vesicles obtained by irradiation of vesicles of trans-PEG550-TPE-Chol (C) and of cylindrical micelles of cis-PEG550-TPE-Chol (D) after 30 min of irradiation by UV light (365 nm, 15 mW/cm2).

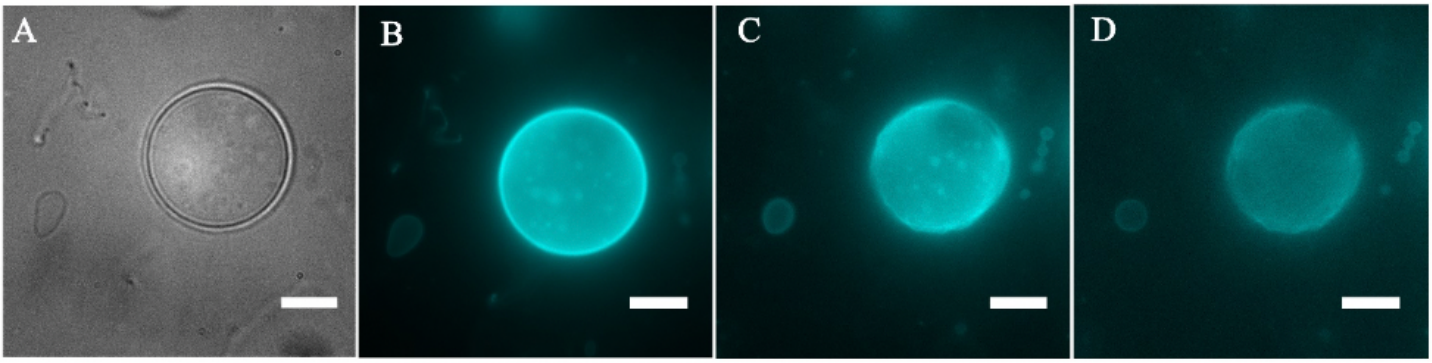

Figure 6

Epifluorescence optical microscopic images of giant vesicles of PEG550-TPE-Chol. (A) White field. (B-D) Fluorescence images under continuous UV illumination at t = 0 (B), t = 40 sec (C) and t = 60 sec (D). The exposure time of each picture was 300 μsec. Scale bar = 10 μm. LED-UV (365 nm) was used for illumination. The focused intensity on the sample was 15 mW/cm2.

Supplementary Files

This is a list of supplementary files associated with this preprint. Click to download.

- LightgatednanoporouspolymersomesfromstereoisomerdirectedselfassembliesSIsubmission.docx